

Numerical Simulation Research on the Residual Stress of Welding on In-Service Gas Pipeline

Yaping Ding^{1, a}, Daiying Yuan^{1, b}, Xiaolin Xu^{2, c}, Yanan Cui^{2, d}

¹ Department of Transportation and Municipal Engineering, Sichuan College of Architectural Technology, Chengdu 610399, China;

² China Petroleum and Gas Pipeline Science Research Institute Co., Ltd., Langfang 065000, China.

^a471253219@qq.com, ^b158673531@qq.com, ^c944650428@qq.com, ^d41100681@qq.com

Abstract

The residual stress induced by the surfacing and fillet welding processes during the in-service welding on the gas pipeline was researched. A 3D thermo-mechanical finite element method with boundary conditions was developed by a same numerical model. The results show that the hoop residual stress along the circumference on the outer surface is higher for fillet than surfacing. However, the residual stress along the axial direction is slightly affected by the adopted welding schemes. At the weld zone, the hoop and axial residual stresses fluctuated and quickly reversed sign from compression to tension.

Keywords

In service welding, Temperature field, Residual stress, Gas pipeline, Surfacing and fillet processes.

1. Introduction

Many accidents occur with the deployment of gas pipeline. Welding onto the gas pipeline is a repair method which can reinstate the pipeline's function without interrupting its operation. It does not only prevent the pollution from leaking in time, but also avoids disrupting pipeline operation and secures continuous gas supply [1, 2].

The burn-through and hydrogen-induced crack were the problems of the in service welding on gas pipeline [3]. When the heat input was increased, the risk of hydrogen-induced crack is decreased, but the risk of burn-through was improved, and the vice versa [4, 5]. It was found that the two problems were induced by the temperature and can be avoided by welding procedure. However, the residual stress of welding has great effect on the performance of in service welding of pipeline. It need to be pay more attention [6, 7].

2. Governing Equations

During the in-service welding, the governing equation for transient heat transfer analysis is:

$$\left\{ \frac{\partial}{\partial x} \left[k(T) \frac{\partial T}{\partial x} \right] + \frac{\partial}{\partial y} \left[k(T) \frac{\partial T}{\partial y} \right] + \frac{\partial}{\partial z} \left[k(T) \frac{\partial T}{\partial z} \right] \right\} + \dot{Q}(T, t) = \rho(T) C_p(T) \frac{\partial T}{\partial t} \quad (1)$$

Where x, y, z are the coordinates in the reference system, t and T are the time and temperature, respectively, \dot{Q} denotes the internal heat generation, ρ is the density, k represents the thermal conductivity and C_p is the specific heat.

The relation between stress and strain is as following:

$$d\sigma_{ij} = D_{ijkl} \left(d\varepsilon_{kl} - d\varepsilon_{kl}^p - d\varepsilon_{kl}^c - d\varepsilon_{kl}^T \right) \quad (2)$$

Where D_{ijkl} denotes the coefficient of elastic tensor, and $d\varepsilon_{pt}$, $d\varepsilon_{pt}^p$, $d\varepsilon_{pt}^c$, $d\varepsilon_{pt}^T$ are the total strain, plastic strain component, creep strain component, and thermal strain component, respectively.

3. Simulation Model

As shown in Fig. 1, each all-around bead for the sleeve was finished by two welders. The welding bead A1 and B1 were welded by two welders simultaneously. After that, the welding bead A2 and B2 were completed. As shown in Fig.2, the surfacing and fillet welding process were designated as the welding scheme #1 and #2, respectively. The in-service welding parameters is listed in Table 1.

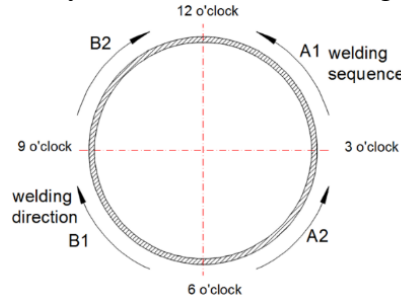


Fig. 1. Welding sequence of all-around bead.

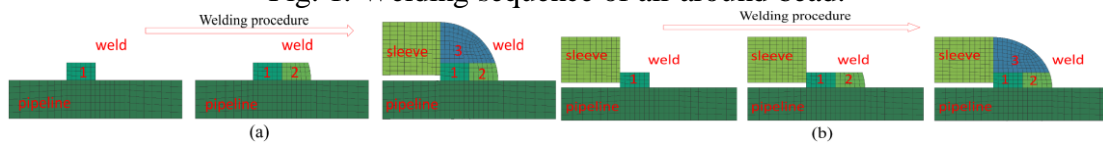


Fig. 2. Welding schemes considered in the present work (a) welding scheme #1 (b) welding scheme #2

Table 1.Parameters of in service welding procedure

Bead No.	Electrode diameter (mm)	Welding current (A)	Arc voltage (V)	Welding speed (cm/min)
1-2	3.2	120-135	24-26	10.8
3	4.0	140-180	25-30	12

Because of structural symmetry, a quarter of sleeve geometry was used for modeling to reduce the number of elements and control the scale of calculation [8]. The mesh size was refined in and near the welding region which shown in Fig 3. The outside diameter of pipe and sleeve is 234 mm and 254 mm, respectively. To compare different welding processes, the same finite element mesh used in the thermal analysis was employed in the thermal and mechanical analysis. The thermal-physical properties of 316L was listed in Table 2.

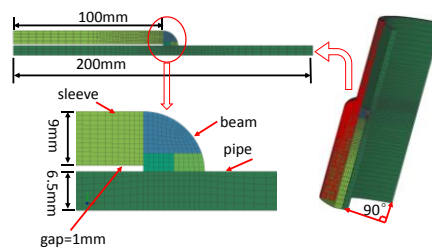


Fig. 3. The FE model and size

Table 2 .Thermal properties of 316L

Temperature (°C)	Density (kg/m ³)	Conductivity W/(m·°C)	Specific heat (J/(kg·°C))	Thermal expansion coeff. (mm/(mm·°C))
20	7979	13.31	0.47	15.24
100	7937	14.68	0.487	15.8
500	7760	20.96	0.571	17.85
1000	7535	27.53	0.676	19.38
1200	7430	29.76	0.719	19.95
1400	7320	31.95	0.765	20.6
1500	7320	320	0.765	20.7

Table 3. Thermal-physical data of fluid medium in pipe.

Flow medium	T (°C)	P (MPa)	ρ (kg/m ³)	c (kJ/(kg·K))	$\lambda \times 10^{-2}$ (W/(m·K))	$\mu_f \times 10^{-6}$ (Pa·s)	v (m/s)
CH ₄	20	1.6	10.9	2.284	3.211	11	10

4. Itribution of Residual Stress

A distribution of series nodes in Path A and Path B was given in Fig 4. The Path A was along the axial direction, which located at the centerline of the weld. The Path B was along the circumferential direction. To compare the difference of the residual stress, both the inner surface and outer surface of the paths were considered.

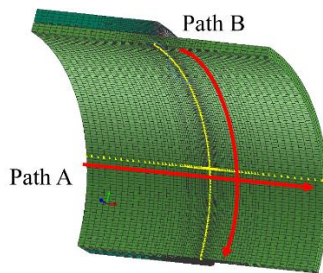


Fig. 4. The stress path along axial direction and circumferential direction

As Fig 5 shown, for both the two welding Schemes, the hoop residual stress increases with the increasing of the angle from the weld start. The maximum hoop residual stress on the inner surface of the pipeline is 578.4 MPa and 531 MPa for welding scheme #1 and #2, respectively. While it is correspondently reduced by 294.5 MPa and 201.5 MPa on the outer surface. The axial residual stress along Path B is plotted in Fig 6. At the weld start point, the axial residual stresses are higher than those of other angles both on outer and inner surface for the two schemes.

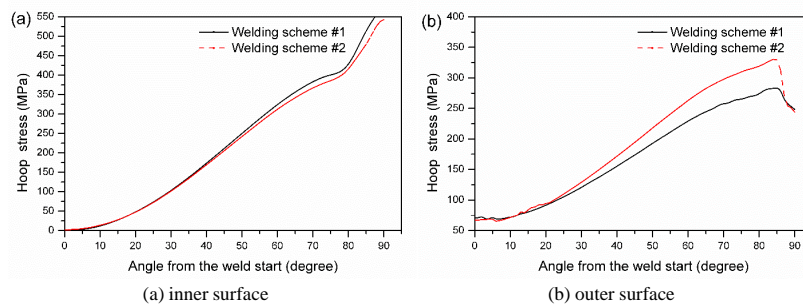


Fig. 5. The hoop stress distribution along Path B (a) inner surface (b) outer surface

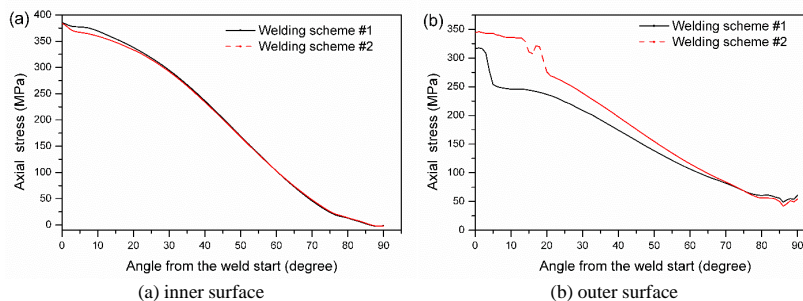


Fig. 6. The axial stress distribution along Path B (a) inner surface (b) outer surface

As shown in Fig 7 -8, the hoop and axial residual stresses of the two schemes fluctuated and quickly reversed sign from compression to tension both on the inner and outer surface of the pipeline at the weld location. It is significantly different from other residual stress along Path A that the axial residual stress on the inner surface is no more than 15 MPa, which was less harmful for the safe of the pipeline.

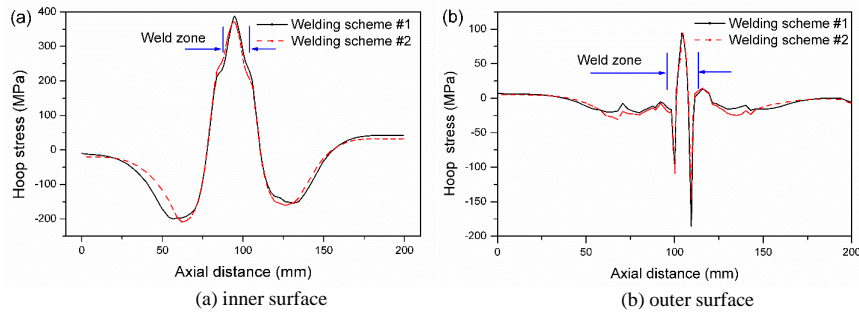


Fig.7. The hoop stress distribution along Path A (a) inner surface (b) outer surface

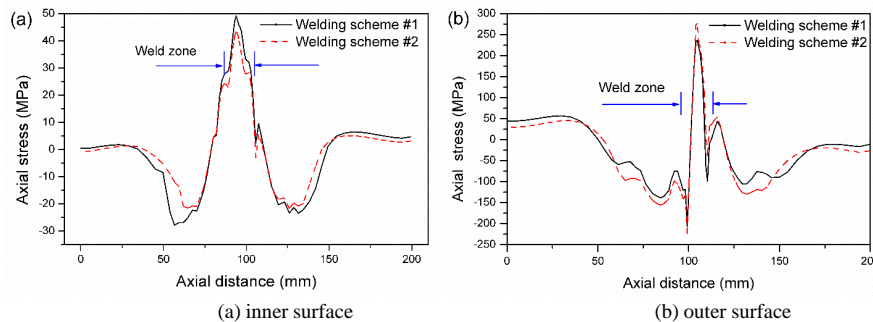


Fig. 8. The axial stress distribution along Path A (a) inner surface (b) outer surface

5. Conclusion

- (1) With the increase of the angle, on the one hand, the hoop residual stress increased, while the axial residual stress decreased; on the other hand, the residual stress of surfacing is higher than that of fillet on the inner surface, but it is opposite on the outer surfacing.
- (2) At the weld zone, the hoop and axial residual stress fluctuated and quickly reversed sign from compression to tension both on the inner and outer surface. The maximum residual stress along the axial direction is located in weld zone. It is obvious that the axial residual stress along axial direction on the inner surface is no more than 15 MPa for both schemes.
- (3) The maximum residual stress on the inner surface is 502.6 MPa for surfacing welding process and 462.6 MPa for fillet welding process. The fillet welding process is a better process.

Acknowledgements

The authors acknowledge the financial supported by the Sichuan College of Architectural Technology 2017KJ14.

References

- [1] Cisilino A.P., Chapetti M.D., Otegui J.L. Minimum thickness for circumferential sleeve repair fillet welds in corroded gas pipelines. *International Journal of Pressure Vessels and Piping*. 2002, 79: 67-76.
- [2] Xue X.L., Sang Z., Zhu J., et al. Numerical simulation of in-service welding of a pressurized pipeline. *Journal of Pressure Vessel Technology, Transactions of the ASME*. 2007, 129: 66-72.
- [3] Asl H.M., Vatani A. Numerical analysis of the burn-through at in-service welding of 316 stainless steel pipeline. *International Journal of Pressure Vessels and Piping*. 2013, 105–106: 49-59.
- [4] Huang Z.Q., Tang H.P., Ding, Y.P., et al. Numerical Simulations of temperature for the in-service welding of gas pipeline. *Journal of Material Processing Technology*. 2017, 248: 72-78.
- [5] *Welding Handbook*. 2004. 9th ed., vol.2 AWS, Miami.

- [6] Fu G., Louren O. M.I., Duan, M., et al. Influence of the welding sequence on residual stress and distortion of fillet welded structures. *Marine Structures*, 2016, 46:30-55.
- [7] Alian, A.R., Shazly, M., Megahed, M.M. 3D finite element modeling of in-service sleeve repair welding of gas pipelines. *International Journal of Pressure Vessels and Piping*. 2016,146, 216-229.
- [8] Deng D., Murakawa H., Numerical simulation of temperature field and residual stress in multi-pass welds in stainless steel pipe and comparison with experimental measurements. *Computational Materials Science*. 2006, 37: 269-277.